Higher order nuclear organization in growth arrest of human mammary epithelial cells: A novel role for telomere-associated protein TIN2

Patrick Kaminker[1], Cedric Plachot[2], Sahn-Ho Kim[3], Peter Chung[3], Danielle Crippen[1], Ole W. Petersen[4], Mina J. Bissell[3], Judith Campisi[1,3] and Sophie A. Lelièvre[2,*].

[1] *Buck Institute for Age research, 8001 Redwood Blvd, Novato, California 94945, USA;* [2]*Department of Basic Medical Sciences and Cancer Center, Purdue University, 625 Harrison Street, West Lafayette, Indiana 47907-2026, USA;* [3] *Life Sciences Division, Lawrence Berkeley National Laboratory, 1 Cyclotron Road, Berkeley, California, 94720, USA;* [4]*Structural Cell Biology Unit, The Panum Institute, University of Copenhagen, Blegdamsvej 3, DK-2200, Copenhagen, DK*.

* Correspondence should be addressed to S.A.L. at:
Department of Basic Medical Sciences, Purdue University, 625 Harrison Street, LYNN, West Lafayette, Indiana 47907-2026, USA. Telephone: 765 496-7793. Fax: 765 494-0781. Email: lelievre@purdue.edu

Running title: TIN2 controls mammary cell growth arrest

Key words: nuclear structure; three-dimensional culture; breast; morphogenesis; quiescence; heterochromatin protein 1.

Summary

Nuclear organization, such as the formation of specific nuclear subdomains, is generally thought to be involved in the control of cellular phenotype; however, there are relatively few specific examples of how mammalian nuclei organize during radical changes in phenotype, such as those which occur during differentiation and growth arrest. Using human mammary epithelial cells (HMECs) in which growth arrest is essential for morphological differentiation, we show that the arrest of cell proliferation is accompanied by a reorganization of the telomere-associated protein, TIN2, into one to three large nuclear subdomains. The large TIN2 domains do not contain telomeres and occur concomitant with the continued presence of TIN2 at telomeres. The TIN2 domains were sensitive to DNAse, but not RNAse, occurred frequently, but not exclusively near nucleoli, and overlapped often with dense domains containing heterochromatin protein 1γ. Expression of truncated forms of TIN2 simultaneously prevented the formation of TIN2 domains and relaxed the stringent morphogenesis-induced growth arrest in HMECs. Our findings reveal a novel extra-telomeric organization of TIN2 associated with the control of cell proliferation and identify TIN2 as an important regulator of mammary epithelial differentiation.

Abbreviations used:

3-D, three-dimensional; BM, basement membrane; DNAse, deoxyribonuclease; ECM, extracellular matrix; EGF, epidermal growth factor; FISH, fluorescence in situ hybridization; HMEC, human mammary epithelial cell; HP 1, heterochromatin protein 1; PML, promyelocytic leukemia protein; RNAse, ribonuclease; TRF1 and 2, telomere-binding factors 1 and 2

Introduction

Changes in higher order nuclear organization may be a key event in the control of cellular phenotypes, particularly the changes in phenotype that occur during development and differentiation (reviewed in Lelièvre et al., 2000; Müller and Leutz, 2001). In lower eukaryotes, telomeres are among the nuclear structures that have been shown to undergo higher order organization, which is important for cell phenotype. Telomeres are the repetitive DNA sequence and specialized proteins that cap the ends of linear chromosomes, and prevent their recombination or degradation by DNA repair processes. Telomeres have long been recognized as important nuclear organizers and regulators of cell phenotype in yeast (Gotta and Gasser, 1996). Specifically, yeast telomeres and their associated proteins organize into clusters at the nuclear periphery, and this clustering is associated with the formation of chromatin domains that determine the pattern of gene expression (Maillet et al., 1996; Gotta et al., 1996). In the somatic cells of higher eukaryotes, however, telomeres are generally randomly distributed throughout the nucleus, and telomeric functions other than their crucial role in chromosome end protection have not been reported.

The structure and function of telomeres depend on the activities of telomere-associated proteins. In mammalian cells, the telomeric end structure is controlled by several telomere-associated proteins, including TRF1, TRF2 and TIN2 (van Steensel and de Lange, 1997; Kim et al., 1999; Kim et al., 2003a). TRF1 and TRF2 bind exclusively to the double-stranded telomeric repeat sequence (Chong et al., 1995; Bilaud et al., 1997), and as such constitute primary telomere-associated proteins. These proteins are thought to function by promoting a closed or capped end structure that protects the chromosome ends from being recognized as 'broken' DNA; these proteins are also thought to negatively regulate telomere length by limiting the

access of telomerase, the reverse transcriptase that can add telomeric DNA repeats to chromosome ends de novo. TIN2 also participates in chromosome end protection (Kim et al., 2004) and negatively regulates telomere length, although it does not bind telomeric DNA directly (Kim et al., 1999). Rather, TIN2 binds TRF1 (Kim et al., 1999) and indirectly influences telomere structure, possibly by altering the conformation of TRF1 (Kim et al., 2003a). In addition, TIN2 binds the telomeric proteins TRF2 and PTOP, also known as PIP1 (Kim et al., 2004; Liu et al., 2004; Ye et al., 2004). Thus, TIN2 is a secondary telomere-associated protein. To date, yeast homologues of TIN2 have not been identified (Kim et al., 1999; Kim et al., 2003b), and the full range of TIN2 functions in mammalian cells is not yet known.

The functional differentiation of the mammary epithelium depends on the growth arrest and proper arrangement of the epithelial cells into glandular structures termed acini. Among the intracellular alterations that are crucial for mammary epithelial cell differentiation, the role of nuclear reorganization is the least well understood and has been only sporadically investigated. We have shown that acinar differentiation entails the redistribution of nuclear proteins such as heterochromatin-associated protein H3K9m, splicing factor SRm160, and the nuclear mitotic apparatus protein NuMA (Lelièvre et al., 1998; Plachot and Lelièvre, 2004). Conversely, we have demonstrated that altering the distribution of NuMA in acinar cells perturbs their differentiation (Lelièvre et al., 1998). These findings suggest that the spatial organization of nuclear components may play an important role in controlling the phenotype of mammalian cells.

Given the importance of telomere organization in controlling gene expression in yeast, and the importance of nuclear organization in the differentiation of human mammary epithelial cells (HMECs), we asked whether the organization of telomeres and/or their associated proteins was important for the control of mammary epithelial phenotypes. To do so, we used three-

dimensional (3-D) cell culture models that recapitulate many aspects of HMEC differentiation. We show that TIN2 undergoes a striking reorganization into large nuclear domains when HMECs arrest proliferation, a prerequisite for acinar differentiation. The formation of large TIN2 domains is not accompanied by clustering of telomeres or TIN2 binding partners, the telomeric proteins TRF1 and TRF2. In addition, both formation of large TIN2 domains and mammary cell growth arrest are impaired upon expression of truncated forms of TIN2. Our findings reveal a higher order nuclear organization associated with growth arrest and define a novel nuclear organizing principle in mammalian cells based on the distribution of telomere-associated proteins.

Materials and Methods

Cell culture and differentiation

HMT-3522 non-neoplastic (S1) HMECs (Briand et al., 1987) were cultured in serum-free H14 medium (GIBCO BRL, St. Louis, MO) as described (Petersen et al., 1992). 184 HMECs, cultured in MCDB 170 medium (Cambrex Biosciences, Walkersville, MD) as described (Hammond et al., 1984), are termed post-selection HMECs because they spontaneously overcame the p16-mediated cell-cycle arrest of primary HMECs (Yaswen and Stampfer, 2002). To induce differentiation, cells were cultured for 10 days on tissue culture surfaces coated with 40 μl/cm^2 Matrigel^{TM} (BD Biosciences, Bedford, MA), a laminin-rich extracellular matrix (ECM); and in culture medium containing 5% Matrigel (Plachot and Lelièvre, 2004). Culture in collagen I was performed as described (Weaver et al., 2002). Briefly, cells were embedded in a collagen mixture (DMEM/F12, 0.1 M Hepes, 0.04 M NaHCO3, cellagen solution AC-5 [ICN Biomedicals Inc, Aurora, OH] diluted 1:4, pH 7.4). Multicellular structures were removed from

the collagen gel by incubating with collagenase D (Roche, Indianapolis, IN) for 30 min at 37°C.

Synchronization of 184 cells

184 HMECs were synchronized as described (Stampfer et al., 1993). Briefly cells were cultured in MEGM medium (Clonetics, La Jolla, CA) supplemented with transferrin (5 μg/ml) and isoproterenol (10^{-5}M) (Sigma, St Louis, MO) and seeded at 50% confluence. Cells were allowed to recover from plating for 24 hrs, rinsed twice in PBS, and then given MEGM lacking EGF and supplemented with 8 μg/ml EGF blocking antibody (MAb 225, American Type Culture Collection hybridoma clone # HB-8508). After 48 hrs, cells were either processed for immunostaining (G0 phase) or released from growth-arrest by washing twice with PBS and replacing the medium with MEGM supplemented with 25 ng/ml EGF and then immunostained at 16 and 20 hrs (S and G2/M phases).

Retroviral infections

Production of retroviruses that express wild type or truncated TIN2 proteins has been described (Kim et al., 1999). We added a C-terminal V5 epitope tag by PCR to create TIN2-V5 and cloned the fragment into the same retroviral vector (pLXSN). Proliferating S1 or 184 HMECs (25-30% confluent) were infected for 6 hrs each on 3 consecutive days with viruses expressing either TIN2-V5, TIN2-13, myc-TIN2-15 (Kim et al., 1999), hTERT (Counter et al., 1998) or GFP, and selected in 200 μg/ml G418 (Invitrogen Life technologies, Carlsbad, CA). hTERT expression was verified by TRAP assay (Chemicon, Temecula, CA), GFP expression was verified by fluorescence microscopy, and wild type and mutant TIN2 expression was verified by western analysis, immunofluorescence, and analysis of telomere length.

Western blot analysis

Total protein extracts were prepared in Laemmli buffer containing 2% sodium dodecyl sulfate. For TIN2 and TIN2-13 expression analysis, 30 μg of protein were separated on 4-12% polyacrylamide gradient gels (Invitrogen), and transferred to a nitrocellulose membrane. The membrane was blocked and incubated with rabbit polyclonal anti-TIN2 antibody that recognizes both full length TIN2 and N-terminally truncated TIN2-13, followed by secondary antibody, as described (Kim et al., 1999). Horseradish peroxidase-conjugated secondary antibody was detected by enhanced chemiluminescence (Amersham Biosciences, Pistacaway, NJ).

Analysis of telomere length

Genomic DNA was isolated from HMECs S1 cells infected with insertless vector, TIN2-13, or TIN2-15 constructs, digested with *Hinf*I and *Rsa*I, and analyzed by Southern blotting using a telomere $(TTAGGG)_3$ probe as described (Harley et al., 1990; Kim et al., 1999). Mean terminal restriction fragment lengths were determined using a phosphorimager (Amersham Biosciences) and ImageQuaNT software (Harley et al., 1990).

Immunofluorescence analysis

Monolayer or 3-D cultures in 4-well chamber slides (Nalge Nunc International, Naperville, IL) were either permeabilized with 0.5% peroxide and carbonyl-free triton X-100 (Sigma Biosciences) in cytoskeleton buffer (100 mM NaCl, 300 mM sucrose, 10 mM pipes, pH6.8, 5 mM MgCl2, 1 mM pefabloc, 10 μg/ml aprotinin, 250 μM NaF) prior to fixation in 4% paraformaldehyde (Sigma Biosciences), or fixed with 4% paraformaldehyde prior to immunostaining (Lelièvre et al., 1998). In some experiments, 3-D cultures were embedded in sucrose, frozen in Tissue-Tek OCT (Sakura Finetek, Torrance, CA), and 5-20 μm frozen sections

were cut and used for immunostaining. Primary antibodies were mouse monoclonal anti-PML (Santa Cruz Biotechnology, Santa Cruz, CA), anti-TRF1 (Oncogene Research Products, San Diego, CA), anti-TRF2 (Imgenex, San Diego, CA), anti-nucleolin (Santa Cruz Biotechnology), anti-HP 1γ (Chemicon), anti-c-myc (clone 9E10, Roche), and rabbit polyclonal anti-TIN2 (Kim et al, 1999). Nuclei were counterstained with 4', 6-diamidino-2-phenylindole (DAPI) or propidium iodide.

Normal human breast biopsies were obtained from women undergoing reduction mammoplasty for cosmetic reasons. The use of human material has been reviewed by the Regional Scientific-Ethical Committees for Copenhagen and Frederiksberg, Denmark and approved with reference (KF) 01-161/98. Tissue cryosections were dried for 15 min at room temperature, incubated for 5 min in 0.5% triton-X 100 in PBS and fixed in 2% paraformaldehyde. After blocking with 10% goat serum, sections were incubated overnight with TIN2 antibody or pre-immune serum from the same rabbit (1:100 in PBS with 10% goat serum), and then for 60 min with FITC-conjugated anti-rabbit IgG. Sections were counterstained with 1 μg/ml propidium iodide.

Immunocytochemistry (ICC) and Fluorescence In Situ Hybridization (FISH)

We used a modification of a FISH assay established to preserve initial ICC staining (Lansdorp et al., 1996). ICC was performed as described above. Following secondary antibody incubation and washing, cells were post-fixed with 4% paraformaldehyde in PBS, washed three times for 5 min each with PBS, dehydrated in ethanol, and air-dried. An 18-mer biotinylated-$(C_3\ TA_2)_3$ peptide-nucleic acid (PNA) probe (Applied Biosystems, Framingham, MA) was hybridized as described (Lansdorp et al., 1996). Following hybridization, samples were incubated with 0.5

μg/ml fluorescein-conjugated streptavidin, counterstained with DAPI, and mounted in anti-fade medium (Vector Laboratories, Burlingame, CA).

Growth analyses

Cells cultured in 3-D for 6 or 10 days were assayed for 5-bromo-2-deoxyuridine (BrdU) incorporation using a commercial labeling and detection kit (Roche). The BrdU-labeling index was determined by scoring 200-400 DAPI-stained cells for BrdU positivity in 4 independent experiments. In parallel experiments, the sizes of acini were analyzed by measuring their diameter using a scaled eye-piece.

DNAse I and RNAse A treatments

Cells were permeabilized using 0.5% peroxide and carbonyl-free triton X-100 (Sigma Biosciences) in the presence of protease and phosphatase inhibitors (PI) in cytoskeleton (CSK) buffer [100mM NaCl; 300mM sucrose; 10mM Pipes, pH6.8; 5mM $MgCl_2$], then incubated with 130 μg/ml DNAse I (Worthington Biochemical Corporation, Lakewood, NJ) or 100 μg/ml DNAse-free RNAse A (Roche) in PI-CSK for 30 min at 37° C. Cells were then fixed as described for immunostaining.

Results

TIN2 organizes into large nuclear domains during HMEC acinar differentiation

To understand whether and how telomeres and/or their associated proteins might influence mammalian cell phenotypes, we followed the localization of telomeres and primary and secondary telomere-associated proteins during the morphological differentiation of HMECs in 3-D culture. The differentiation of HMECs under these conditions is accompanied by an arrest of cell proliferation (Petersen et al., 1992; Lelièvre et al., 1998), chromatin remodeling and changes in gene expression (Bissell et al., 2003; Plachot and Lelièvre, 2004). We initiated our studies using the non-neoplastic human breast epithelial cell line, HMT-3522 (S1), which forms tissue-like acini when cultured in the presence of Matrigel in 3-D. During the 10-day morphogenesis process, S1 cells proliferate for 5-6 days, then arrest growth, deposit an endogenous basement membrane (BM), and polarize around a central lumen (Petersen et al., 1992).

We immunostained proliferating and differentiated S1 cells for telomere-associated proteins including TIN2, Ku, ATM, TRF2, and TRF1. Among these proteins, only TIN2 showed a dramatic redistribution upon completion of acinar differentiation (Fig. 1A).

In human fibroblasts, TIN2 localizes exclusively to telomeres, which appear randomly distributed as small foci throughout the nucleus (Kim et al., 1999). TIN2 showed a similar random punctate pattern in the nuclei of proliferating S1 cells cultured as monolayers. However, when S1 cells underwent acinar differentiation in 3-D culture, TIN2 reorganized into large domains (Fig. 1A). Each nucleus contained one to three large TIN2 domains that co-existed with the small foci seen in monolayer cultures. The small TIN2 foci most likely corresponded to telomeres, which remained dispersed throughout the nuclei after differentiation, as determined by separate staining for telomeres using a PNA telomeric probe or immunostaining for primary

telomere-associated proteins TRF1 or TRF2. It was not possible to co-stain 3-D cultures for telomeres and TIN2 owing to high non-specific signals from the Matrigel after fixation. However, sectioning of 3-D culture of acini followed by FISH using the telomeric PNA probe showed that the telomeres did not cluster after differentiation (Fig. 1A). Thus, TIN2 remained at telomeres upon differentiation, but additionally clustered into large nuclear domains. These domains did not result from the clustering of either telomeres or the TIN2 telomeric binding partners TRF1 and TRF2.

We detected large TIN2 domains in >80% of the nuclei present in S1 acini. We detected TIN2 only as small foci that overlapped with telomere-binding protein TRF2 in proliferating finite life span HMECs, strain 184 (Hammond et al., 1984; Yaswen and Stampfer, 2002) (see Fig. 1C). However, similarly to S1 cells, large TIN2 domains were observed in the majority of 184 cells that arrested proliferation and underwent morphological differentiation in 3-D culture (see Fig. 1D, discussed below). Moreover, we detected large TIN2 domains in biopsies from normal human breast tissue, where many of the epithelial cells in the acini showed clustered TIN2 immunostaining (Fig. 1B). Thus, the formation of large TIN2 domains was not unique to S1 cells, and was not restricted to cultured cells.

To confirm that the large domains recognized by our affinity-purified antibody indeed correspond to TIN2, we expressed a C-terminally V5-epitope-tagged TIN2 protein in 184 HMECs using retroviral transduction. We allowed the cells to form acini in 3-D culture, then dually stained with V5 and TIN2 antibodies. The antibodies showed >95% co-localization, identifying TIN2 in both small foci and large domains (Fig. 1D). We conclude that TIN2 organizes into large domains when HMECs undergo morphological differentiation.

TIN2 domains are frequently perinucleolar and associated with HP 1γ

To determine whether large TIN2 domains overlap with other nuclear structures, we performed dual immunostaining for TIN2 and the nucleolar protein nucleolin. Whereas TIN2 domains did not co-localize with nucleoli, they frequently (>55%) were perinucleolar (Fig. 2A). Since nucleoli are sites of intense RNA metabolism and are also linked to gene silencing (Olson et al., 2002), we asked whether integrity of the large TIN2 domains depended on intact RNA- or DNA-rich structures. We used PML as a control because its distribution into distinct domains is not dramatically altered upon RNAse A or DNAse I treatment (Szekely et al., 1999). TIN2 domains did not substantially overlap with PML domains, which contain proteins that participate in a variety of cellular processes including transcription (Borden, 2002). Moreover, RNAse A treatment left both the PML and TIN2 domains intact (Fig. 2B), but DNAse I treatment markedly and selectively eliminated the large TIN2 structures (Fig. 2B). This finding raised the possibility that the large TIN2 domains associate with chromatin, since disappearance of protein domains following DNAse I treatment is considered a good indicator that such domains are part of DNA-rich regions (Szekely et al., 1999). This possibility was supported by staining acini for both TIN2 and heterochromatin protein HP 1γ, which is known to participate in chromatin packaging and gene silencing (Li et al., 2002) (Fig. 2C). HP 1γ was widely but unevenly distributed throughout the nucleus, showing areas of relatively light staining, as well as regions of dense focal staining. The majority (80%) of large TIN2 domains co-localized with dense focal HP 1γ staining. These findings suggest that TIN2 may participate in organizing chromatin during breast acinar differentiation, a possibility we are currently investigating in greater detail.

Formation of large TIN2 domains coincides with arrest of cell proliferation

Morphological differentiation into acini entails an arrest of cell proliferation, in addition to the formation of a polarity axis (Petersen et al., 1992; Weaver et al., 1997; Lelièvre et al., 1998). To

determine whether the formation of large TIN2 domains was associated with polarity or growth arrest, we cultured S1 cells in collagen I, rather than the laminin-rich Matrigel. Under these conditions, the cells arrest proliferation, form multicellular structures of sizes similar to the acini formed in Matrigel, but the cells inversely polarize (Gudjonsson et al., 2002; Weaver et al., 2002). Large TIN2 domains were present in the majority of nuclei when S1 cells were cultured for 10 days in collagen I (Fig. 3A). Thus, formation of large TIN2 domains did not depend on acinar polarity.

We next asked whether growth arrest was necessary for the formation of large TIN2 domains. We cultured S1 and 184 HMECs as subconfluent monolayers in a defined medium, then arrested proliferation by providing medium lacking EGF. After three days, most of the cells withdrew from the cell cycle (Lelièvre et al., 1998; not shown), and TIN2 formed large domains in about 80% of the nuclei (Fig. 3A-B). S1 cells also arrested proliferation upon reaching confluence, even in the presence of EGF, and TIN2 formed large domains in the majority of confluent S1 cells (not shown). Thus, the formation of large TIN2 domains was associated with growth arrest, rather than an absence of EGF or acinus formation per se.

Consistent with our observations in 3-D cultures, the TIN2 domains that formed upon growth arrest in monolayer cultures frequently localized adjacent to nucleoli (Fig. 3B) and partially or totally overlapped with HP 1γ domains (Fig 3C). To more definitively determine the relationship between large TIN2 domains and telomeres, we co-stained growth-arrested S1 monolayer for telomeres and TIN2. Although occasional telomeric foci could be observed within a large TIN2 domain, most of the large TIN2 domains were devoid of telomeres and most of the telomeres were outside the large TIN2 domains (Fig. 4A). Dual staining for TIN2 and TRF1 or TRF2 likewise showed that only TIN2 formed large domains in growth-arrested cells (Fig. 4A), and that the majority of TRF1 and TRF2 focal staining was excluded from these

domains. The foci-like distribution of TIN2 outside large domains overlapped with TRF2, a marker of telomeres, indicating that TIN2 remains at telomeres in growth-arrested cells but additionally forms large domains outside the telomeres (Fig. 4B).

To more accurately define the cell-cycle dependence of TIN2 domain formation, we co-stained S1 cells for TIN2 and Ki-67, a cell proliferation marker that displays distinct nuclear distributions depending on the phase of the cell cycle (Braun et al., 1988). In proliferating cells (day 3 of 3-D culture or monolayers in the presence of EGF), ~30% of cycling (Ki-67 positive) cells displayed large TIN2 domains. By contrast, ~80% of non-cycling (Ki-67 negative) cells displayed large TIN2 domains (Fig. 5A). Examination of the Ki-67 staining pattern and TIN2 distribution showed that large TIN2 domains were present primarily during the G0 and G1 phases of the cell cycle, whereas only a few cells in S phase, and virtually no cells in the G2 and M phases, had these large domains (Fig. 5B). To confirm that large TIN2 domains form primarily in G0 and G1, we synchronized 184 HMECs in monolayer culture by incubating in medium lacking EGF and supplemented with EGF blocking antibody. We immunostained the cells for Ki-67 and TIN2 while growth-arrested, as well as 16 and 20 hours after release from growth arrest, which corresponded to the mid-S and G2/M phases of the cell cycle, respectively, as confirmed by Ki-67 staining. The majority of 184 cells displaying large TIN2 domains were negative for Ki-67 (Fig. 5C). Thus, TIN2 formed large domains primarily when cells were quiescent.

Truncated forms of TIN2 prevent formation of large TIN2 domain and growth arrest

To determine whether the change in TIN2 organization is related to the status of growth in HMECs, we infected S1 cells with retroviruses expressing either N-terminally (TIN2-13)- or C-terminally (TIN2-15) truncated forms of TIN2 (Fig. 6A). These mutants interfere with the

telomere length control function of wild type TIN2 in a dominant negative fashion (Kim et al., 1999). Viruses lacking an insert (vector control), expressing green fluorescent protein (GFP) or expressing hTERT (catalytic subunit of human telomerase) served as controls for the effects of infection, expression of an ectopic protein, and expression of a telomeric protein that does not interact with TIN2, respectively. Western analysis confirmed expression of TIN2-13 (Fig. 6B). However, because our polyclonal antibody was raised against an N-terminally truncated protein, TIN2-15 was undetectable by western analysis. In addition, detection of TIN2-15 in protein extracts using an antibody against the myc-epitope tag was marginal, indicating that TIN2-15 is unstable or the anti-myc antibody does not detect this protein readily on western blots. However, TIN2-15 was detectable in cell nuclei in monolayer and 3-D cultures by anti-myc immunostaining (Fig. 6C). To confirm the expression of both truncated proteins, we performed Southern analysis using a telomeric probe to assess the effect of TIN2-13 and TIN2-15 on telomere length (Kim et al., 1999). Cells infected with either TIN2-13 or TIN2-15 constructs showed a 27% and 46% increase in mean telomere length, respectively, compared to vector control after seven population doublings, indicating that both TIN2 mutants were expressed and biologically active.

In contrast to control cells, cells that expressed TIN2-13 or TIN2-15 formed heterogeneous and disorganized acini. TIN2-15 was more potent than TIN2-13 in this regard (Fig. 6D). TIN2-15-expressing cells formed acini that were up to 4-fold larger than control acini, indicating a loss of growth control. In addition, very few of these acini showed basal localization of collagen IV, indicating loss of acinar polarity (Fig. 6E-F). GFP and hTERT-expressing S1 cells did not display any detectable alteration in acinar morphogenesis (Fig. 6G).

To further investigate the effects of TIN2 mutants on proliferation, we assessed cell cycle activity by Ki-67 immunostaining and BrdU incorporation. After 10 days in 3-D culture, both

TIN2-13- and TIN2-15-expressing S1 cells showed substantially more Ki-67 staining (Fig. 6F) than control cells. Moreover, the sharp drop in BrdU-positive cells usually observed between days 6 and 10 of acinus formation was less pronounced in TIN2-13-expressing cells, and essentially eliminated in TIN2-15-expressing cells (decrease in BrdU positive index: 64.6% +/- 8.8 in control, 52.98% +/- 4.4 in TIN2-13, and 16.6 % +/- 9.8 in TIN2-15). Similarly, TIN2-15-expressing cells cultured as monolayers were resistant to EGF withdrawal-induced growth arrest, as indicated by the high number of BrdU positive cells compared to controls after three days in medium lacking EGF (not shown). Thus, cells expressing mutant forms of TIN2 had a diminished capacity to respond to signals for growth arrest.

To determine whether the TIN2 mutants acted in a dominant negative fashion to prevent the formation of large TIN2 domains, we examined the distribution of TIN2 in TIN2-13- and TIN2-15-expressing cells cultured in 3-D for 10 days. Formation of large TIN2 domains was reduced sharply, approximately 3- and 4.5-fold respectively, in the aberrant acini formed by TIN2-13- and TIN2-15-expressing cells. Thus, nuclei with large TIN2 domains were observed in 80% of control cells, 27% of TIN2-13-expressing cells, and 18% of TIN2-15-expressing cells. Within the disorganized acini, nuclei with prominent TIN2 domains could be seen alongside nuclei devoid of large TIN2 domains or showing only fragmented TIN2 domains (Fig. 6H). Expression of TIN2-15 was not accompanied by the formation of large domains containing TIN2-15 (see Fig. 6C). Thus, the TIN2 mutants greatly diminished formation of large TIN2 domains and prevented efficient growth arrest.

Discussion

Our findings provide the first evidence that a mammalian telomere-associated protein forms a novel nuclear structure, which is not associated with telomeres, and that formation of this structure is important for the growth arrest of HMECs under monolayer and 3-D culture conditions. This protein, TIN2, associates with telomeres indirectly by binding to TRF1 (Kim et al., 1999) and TRF2 (Kim et al., 2004). We show here that TIN2 also forms large non-telomeric domains in a non-neoplastic human mammary epithelial cell line and a finite life span human mammary cell strain. In addition, large TIN2 domains were detectable in normal human breast tissue, indicating that these structures do form in vivo.

The large TIN2 domains observed in mammary epithelial cells were not accompanied by clustering of telomeric DNA or the TIN2 binding partners TRF1 and TRF2 proteins. The clustering or aggregation of telomeric components has been described during spermatogenesis in mammalian cells (Zalensky et al., 1997). In male germ cells, clustering of telomeric DNA is mediated by a telomere-binding protein complex (hSTBP) that includes a variant of histone H2B but does not contain TRF1 or TRF2 (Gineitis et al., 2000). This higher organization of telomeric DNA is established during early meiosis and is proposed to be important for fertilization and early development (Zalensky et al., 1997). In contrast, we have found no evidence for higher order telomere clusters (i.e., large domains that include telomeric DNA) in somatic mammalian cells, in agreement with previous studies (Ludérus et al., 1996) that used tumor-derived and non-transformed mammalian cells. However, these studies did not explore the effects of growth arrest or tissue differentiation on telomere organization. Our results show that although the striking phenotypic changes that accompany acinar morphogenesis do not alter telomere organization, acinar morphogenesis was accompanied by higher order nuclear organization of the secondary

telomere-associated protein, TIN2. Thus, in contrast to the clustering of telomeres in germ cells, our findings suggest that telomere components, but not telomeres, may cluster in somatic cells.

Using a variety of cell culture manipulations, we determined that the important step for the formation of large TIN2 domains was exit from the cell cycle. The importance of the large TIN2 domains for the growth arrest of HMECs was evident from the behavior of cells expressing mutant forms of TIN2. Truncated forms of TIN2 prevented the formation of large TIN2 domains, and simultaneously interfered with the ability of cells to arrest proliferation both in 3-D and monolayer culture. These data suggest that TIN2 reorganization is likely crucial for proper HMEC growth control and hence subsequent acinar differentiation. We do not yet know whether large TIN2 domain formation and its influence on growth arrest occur in multiple cell types, or are restricted to HMECs. Preliminary data suggest that large TIN2 domains do not form naturally in growth-arrested fibroblasts (unpublished data), raising the possibility that their formation is restricted to all or certain types of epithelial cells.

Although dual staining for TIN2 and telomeric DNA could not be achieved in 3-D culture, dual staining on growth-arrested cells in monolayer culture showed that telomeres were not constituents of the large TIN2 domains. These data suggest that there is an extra-telomeric function for TIN2 upon growth arrest of HMECs. It is important to emphasize that the reorganization of TIN2 observed upon growth arrest in HMECs was not associated with loss of TIN2 from telomeres. Rather, the reorganization entailed a gain of TIN2 at mostly perinucleolar sites. The mechanisms that trigger recruitment of TIN2 to extra-telomeric domains in growth-arrested HMECs are not yet understood but may involve binding to as yet unknown partners. Our finding that the large TIN2 domains frequently associate with HP 1γ suggests that TIN2 may be recruited to extra-telomeric sites by chromatin-associated proteins. In support of this possibility, other HP 1 variants have been shown to interact with TRF1/PIN2 in mice and Ku70

in humans (Netzer et al., 2001; Song et al., 2001).

The role of TIN2 within HP 1/TIN2 domains remains to be deciphered. TIN2 domains were DNAse sensitive, suggesting an association with chromatin, and they frequently associated with HP 1γ, a known heterochromatin-associated protein. Therefore, our current hypothesis is that large TIN2 domains may promote chromatin compaction in association with other chromatin components. Indeed the highly conserved HP 1 proteins are key transcriptional regulators and are critical for the functional and structural organization of the nucleus (Kellum, 2003). Notably, the binding of HP 1 variants (including HP 1 γ) to many different proteins indicates a central role for this protein family in nuclear function. Thus, TIN2 may have the capability to organize chromatin, possibly in conjunction with HP 1, although so far TIN2 has only been shown to promote the compaction of telomeric chromatin in association with TRF1 (Kim et al., 2003a). The participation of large TIN2 domains in chromatin compaction is suggested further by the frequent localization of these domains to perinucleolar regions, where heterochromatin and/or regions of gene silencing have been located (Olson et al., 2002).

Chromatin remodeling is a key event in differentiation processes in both non-mammalian and mammalian cells (Müller and Leutz, 2001; Plachot and Lelièvre, 2004). Most interestingly, it was recently demonstrated that alterations in chromatin structure also precede exit from the cell cycle (Barbie et al., 2004): perinucleolar replication foci were shown to persist throughout S phase prior to exit from the cell cycle. In addition, pRB and histone deacetylase complexes localized to perinucleolar replication sites and thus, might be poised to establish repressive chromatin structures in the vicinity of the nucleolus. One possibility is that HP 1 intervenes at this step via its ability to propagate heterochromatin and hence help silence genes that promote cell proliferation. TIN2 may facilitate this process in HMECs by promoting chromatin

compaction due to its influence on a binding partner, similar to its effect on the compaction of telomeric DNA (Kim et al., 2003a). This could result in the formation of a highly dense chromatin structure capable of repressing gene activity. The expression of truncated forms of TIN2, one of which was shown to be defective in telomeric DNA compaction (Kim et al., 2003a), was sufficient to prevent the formation of large TIN2 domains and growth arrest. These results suggest that these TIN2 domains may have a repressive effect on genes that promote proliferation.

Whether telomere organization influences the formation of large extra-telomeric TIN2 domains as well as the function of TIN2 in these large domains is an exciting question. TIN2 is a critical regulator of telomere length, and TIN2-induced changes in telomere length may, in turn, affect telomere organization and the formation of large TIN2 domains. Indeed expression of truncated forms of TIN2 in S1 cells affected both telomere length and the formation of large TIN2 domains. The molecular tools currently available do not allow us to specifically target TIN2 located in the large perinucleolar domains and thus to assess whether the organization of large TIN2 domains is sufficient to control growth arrest. The identification of TIN2 binding partners within the large domains will be critical to address this question.

In yeast, clustering of telomeric DNA and associated proteins influences cellular phenotypes; our findings indicate that mammary epithelial cell phenotypes are influenced by the organization of a secondary telomere-associated protein. It will be of interest to examine other differentiation systems for TIN2 organization and also for the organization of other telomere-associated proteins. Although telomeric sequences tend to be highly conserved across species, mammalian telomeric proteins show significantly greater divergence (Li et al., 2000; de Lange, 2004), suggesting that the telomeric proteins of higher organisms may have functions in addition to telomere protection and regulation of telomere length.

Acknowledgments:

We thank Martha Stampfer and Paul Yaswen for the 184 cells, Robert Weinberg for the hTERT cDNA, Fritz Rank for breast biopsy samples and Tove Marianne Lund for technical assistance. We also thank Carol Prives, Sybille Galosy, and Derek Radisky and in particular Zena Werb for critical reading of the manuscript and insightful comments. This work was supported by the Department of Energy, Office of Health and Environmental Research (DE-AC03 SF0098 to M.J.B. and J.C.), Walther Cancer Institute (WCI-110-114 to S.A.L.), Jim and Diane Robbers Foundation at the Purdue Cancer Center (S.A.L.), California Breast Cancer Research Program (88AV01 to S-H.K.), Danish Research Council and Novo Nordisk Foundation to O.W.P., National Institutes of Health (CA64786 to M.J.B. and AG09909 to J.C.), Department of Defense Breast Cancer Research Program (DAMD17-02-1-0438 to M.J.B.), California Breast Cancer Research Program (7FB0018 to P.K.), Joyce Fox Jordan Cancer Research Program at the Purdue Cancer Center (C.P.), Department of Energy, Undergraduate Laboratory Fellowship program (P.C.), and National Institutes of Health training grant (AG00266).

References

Barbie, D.A., Kudlow, B.A., Frock, R., Zhao, J., Johnson, B.R., Dyson, N., Harlow, E. and Kennedy, B.K. (2004). Nuclear reorganization of mammalian DNA synthesis prior to cell cycle exit. *Mol. Cell. Biol.* **24**, 595-607.

Bilaud, T., Brun, C., Ancelin, K., Koering, C.E., Laroche, T. and Gilson, E. (1997). Telomeric localization of TRF2, a novel human telobox protein. *Nat. Genet*. **17**, 236-239.

Bissell, M.J., Rizki, A. and Mian, I.S. (2003). Tissue architecture: the ultimate regulator of breast epithelial function. *Curr. Opin. Cell. Biol.* **6**,753-62.

Borden, K.L. (2002). Pondering the promyelocytic leukemia protein (PML) puzzle: possible functions for PML nuclear bodies. *Mol. Cell. Biol.* **22**, 5259-5269.

Braun, N., Papadopoulos, T. and Muller-Hermelink, H.K. (1988). Cell cycle dependent distribution of the proliferation-associated Ki-67 antigen in human embryonic lung cells. *Virchows Arch. B. Cell. Pathol. Incl. Mol. Pathol.* **56**, 25-33.

Briand, P., Petersen, O.W. and Van Deurs, B. (1987). A new diploid nontumorigenic human breast epithelial cell line isolated and propagated in chemically defined medium. *In Vitro Cell Dev. Biol.* **23**, 181-188.

Chong, L., van Steensel, B., Broccoli, D., Erdjument-Bromage, H., Hanish, J., Tempst, P. and de Lange, T. (1995). A human telomeric protein. *Science* **270**, 1663-1667.

Counter, C.M., Meyerson, M., Eaton, E.N., Ellisen, L.W., Caddle, S.D., Haber, D.A. and Weinberg, R.A. (1998). Telomerase activity is restored in human cells by ectopic expression of hTERT (hEST2), the catalytic subunit of telomerase. *Oncogene* **16**, 1217-1222.

de Lange, T. (2004). T-loops and the origin of telomeres. *Nat. Rev. Mol. Cell. Biol.* **5**, 323-329.

Gineitis, A.A., Zalenskaya, I.A., Yau, P.M., Bradbury, E.M. and Zalensky, A.O. (2000). Human sperm telomere-binding complex involves histone H2B and secures telomere membrane attachment. *J. Cell Biol.* **151**, 1591-1598.

Gotta, M. and Gasser, S.M. (1996). Nuclear organization and transcriptional silencing in yeast. *Experientia* **52**, 1136-1147.

Gotta, M., Laroche, T., Formenton, A., Maillet, L., Scherthan, H. and Gasser, S.M. (1996). The clustering of telomeres and colocalization with Rap1, Sir3, and Sir4 proteins in wild type Saccharomyces cerevisiae. *J. Cell Biol.* **134**, 1349-1363.

Gudjonsson, T., Rønnov-Jessen, L., Villadsen, R., Rank, F., Bissell, M.J. and Petersen, O.W. (2002). Normal and tumor-derived myoepithelial cells differ in their ability to signal to luminal breast epithelial cells for polarity and basement membrane deposition. *J. Cell Sci.* **115,** 39-50.

Hammond, S.L., Ham, R.G. and Stampfer, M.R. (1984). Serum-free growth of human

mammary epithelial cells: rapid clonal growth in defined medium and extended serial passage with pituitary extract. *Proc. Natl. Acad. Sci. U S A* **81**, 5435-5439.

Harley, C.B., Futcher, C. and Greider, C.W. (1990). Telomeres shorten during ageing of human fibroblasts. *Nature* **345**, 458-460.

Kellum, R. (2003). HP1 complexes and heterochromatin assembly. *Curr. Top. Microbiol. Immunol.* **274**, 53-77.

Kim, S. H., Beausejour, C., Davalos, A. R., Kaminker, P., Heo, S. J. and Campisi, J. (2004). TIN2 mediates functions of TRF2 at human telomeres. *J. Biol. Chem.* **279**, 43799-804.

Kim, S.H., Han, S., You, Y.H., Chen, D.J. and Campisi, J. (2003a). The human telomere-associated protein TIN2 stimulates interactions between telomeric DNA tracts in vitro. *EMBO Rep.* **4**, 685-691.

Kim, S.H., Parrinello, S., Kim, J. and Campisi, J. (2003b). Mus musculus and Mus spretus homologues of the human telomere-associated protein TIN2. *Genomics* **81**, 422-32.

Kim, S.H., Kaminker, P. and Campisi, J. (1999). TIN2, a new regulator of telomere length in human cells. *Nat. Genet.* **23**, 405-412.

Lansdorp, P.M., Verwoerd, N.P., van de Rijke, F.M., Dragowska, V., Little, M.T., Dirks, R.W., Raap, A.K. and Tanke, H.J. (1996). Heterogeneity in telomere length of human

chromosomes. *Hum. Mol. Genet.* **5**, 685-691.

Lelièvre, S.A., Weaver, V.M., Nickerson, J.A., Larabell, C.A., Bhaumik, A., Petersen, O.W. and Bissell, M.J. (1998). Tissue phenotype depends on reciprocal interactions between the extracellular matrix and the structural organization of the nucleus. *Proc. Natl. Acad. Sci.U S A* **95**, 14711-14716.

Lelièvre, S.A., Bissell, M.J. and Pujuguet, P. (2000). Cell nucleus in context. *Crit. Rev. Eukaryot. Gene Expr.* **10**, 13-20.

Li, B., Oestreich, S. and de Lange, T. (2000). Identification of human Rap1: implications for telomere evolution. *Cell* **101**, 471-83.

Li, Y., Kirschmann, D.A. and Wallrath, L.L. (2002). Does heterochromatin protein 1 always follow code? *Proc. Natl. Acad. Sci. U S A* **99**, 16462-16469.

Liu, D., Safari, A., O'Connor, M. S., Chan, D. W., Laegeler, A., Qin, J. and Songyang, Z. (2004). PTOP interacts with POT1 and regulates its localization to telomeres. *Nat. Cell Biol.* **6**, 673-80.

Ludérus, M.E., van Steensel, B., Chong, L., Sibon, O.C., Cremers, F.F. and de Lange, T. (1996). Structure, subnuclear distribution, and nuclear matrix association of the mammalian telomeric complex. *J. Cell Biol.* **135**, 867-81.

Maillet, L., Boscheron, C., Gotta, M., Marcand, S., Gilson, E. and Gasser, S.M. (1996). Evidence for silencing compartments within the yeast nucleus: a role for telomere proximity and Sir protein concentration in silencer-mediated repression. *Genes Dev.* **10**, 1796-1811.

Müller, C. and Leutz, A. (2001). Chromatin remodeling in development and differentiation. *Curr Opin Genet Dev.* **11**, 167-74.

Netzer, C., Rieger, L., Brero, A., Zhang, C.D., Hinzke, M., Kohlhase, J. and Bohlander, S.K. (2001). SALL1, the gene mutated in Townes-Brocks syndrome, encodes a transcriptional repressor which interacts with TRF1/PIN2 and localizes to pericentromeric heterochromatin. *Hum. Mol. Genet.* **10**, 3017-24.

Olson, M.O., Hingorani, K. and Szebeni, A. (2002). Conventional and nonconventional roles of the nucleolus. *Int. Rev. Cytol.* **219**, 199-266.

Petersen, O.W., Ronnov-Jessen, L., Howlett, A.R. and Bissell, M.J. (1992). Interaction with basement membrane serves to rapidly distinguish growth and differentiation pattern of normal and malignant human breast epithelial cells [published erratum appears in Pro. Natl. Acad. Sci. U S A 1993 Mar 15;90(6):2556]. *Proc. Natl. Acad. Sci. U S A* **89**, 9064-9068.

Plachot, C. and Lelièvre, S.A. (2004). DNA methylation control of tissue polarity and cellular differentiation in the mammary epithelium. *Exp. Cell Res.* **298**, 122-132.

Szekely, L., Kiss, C., Mattsson, K., Kashuba, E., Pokrovskaja, K., Juhasz, A., Holmvall, P.

and Klein, G. (1999). Human herpesvirus-8-encoded LNA-1 accumulates in heterochromatin-associated nuclear bodies. *J. Gen. Virol.* **80 (Pt 11)**, 2889-900.

Song, K., Jung, Y., Jung, D. and Lee, I. (2001). Human Ku70 interacts with heterochromatin protein 1alpha. *J. Biol. Chem.* **276**, 8321-7.

Stampfer, M.R., Pan, C.H., Hosoda, J., Bartholomew, J., Mendelsohn, J. and Yaswen, P. (1993). Blockage of EGF receptor signal transduction causes reversible arrest of normal and immortal human mammary epithelial cells with synchronous reentry into the cell cycle. *Exp. Cell Res.* **208**, 175-188.

van Steensel, B. and de Lange, T. (1997). Control of telomere length by the human telomeric protein TRF1. *Nature* **385**, 740-743.

Weaver, V.M., Petersen, O.W., Wang, F., Larabell, C.A., Briand, P., Damsky, C. and Bissell, M.J. (1997). Reversion of the malignant phenotype of human breast cells in three-dimensional culture and in vivo by integrin blocking antibodies. *J. Cell Biol.* **137**, 231-245.

Weaver, V.M., Lelièvre, S., Lakins, J.N., Chrenek, M.A., Jones, J.C., Giancotti, F., Werb, Z. and Bissell, M.J. (2002). beta4 integrin-dependent formation of polarized three-dimensional architecture confers resistance to apoptosis in normal and malignant mammary epithelium. *Cancer Cell* **2**, 205-216.

Yaswen, P. and Stampfer, M.R. (2002). Molecular Changes accompanying senescence and

immortalization of cultured human mammary epithelial cells. *Int. J. Biochem. Cell Biol.* **34**, 1382-1394.

Ye, J. Z., Hockemeyer, D., Krutchinsky, A. N., Loayza, D., Hooper, S. M., Chait, B. T. and de Lange, T. (2004). POT1-interacting protein PIP1: a telomere length regulator that recruits POT1 to the TIN2/TRF1 complex. *Genes Dev.* **18**, 1649-54.

Zalensky, A.O., Tomilin, N.V., Zalenskaya, I.A., Teplitz, R.L. and Bradbury, E.M. (1997). Telomere-telomere interactions and candidate telomere binding protein(s) in mammalian sperm cells. *Exp. Cell Res.* **232**, 29-41

Figure Legends

Fig. 1. Large TIN2 domains are present in HMECs organized into acini. (A) Immunostaining for TIN2 (green) and PNA FISH for telomeres (red) in S1 acini in 3-D culture. (B) Immunostaining for TIN2 (green) in a biopsy from normal breast tissue. (C) Dual immunostaining for TIN2 (red) and TRF2 (green) in the nuclei of proliferating HMECs, strain 184. Co-localization of TIN2 and TRF2 appears yellow. (D) Dual immunostaining for TIN2 (red) and V5 (green) in the nuclei of acini formed by 184 HMECs expressing V5-tagged TIN2 in 3-D culture. Nuclei are counterstained with DAPI (blue) in A, C and D, and propidium iodide (red) in B. Images in B and D are confocal sections of acini containing several nuclei. Arrowheads indicate large TIN2 domains. Size bars = 5 microns.

Fig. 2. Large TIN2 domains are often perinucleolar and co-localized with dense HP 1γ foci. (A) Dual immunostaining for TIN2 (green) and nucleolin (red) in S1 acini in 3-D culture. The image is a confocal section of an acinus containing several nuclei, illustrated by the drawing on the left. (B) Dual staining for TIN2 (green) and PML (red) in S1 acini. 3-D cultures were untreated (control) or treated for 30 min with DNAse I [DNAse] or RNAse A [RNAse] prior to immunostaining. (C) Dual immunostaining for HP 1γ (red) and TIN2 (green) in S1 acini. Arrows indicate HP 1γ domains that overlap with large TIN2 domains, arrowheads indicate large TIN2 domains, and dashed-lines delineate the nuclear periphery. Size bars = 5 microns.

Fig. 3. Formation of large TIN2 domains in growth-arrested cells is independent of the differentiation status. (A) Large TIN2 domains (arrowheads) revealed by immunostaining (red) in correctly polarized S1 cells cultured in 3-D laminin-rich ECM (S1-Matrigel), S1 cells cultured

in 3-D collagen I (S1-Collagen I) that display altered polarity, and growth-arrested (EGF-deprived) S1 cells cultured as a monolayer on plastic. Nuclei are counterstained with DAPI (blue). (B) Immunostaining for TIN2 (yellow) in growth-arrested 184 cells cultured as a monolayer on plastic. The superimposed phase contrast image shows the nucleoli as dark gray subnuclear structures. Arrows indicate large TIN2 domains located next to nucleoli. (C) Dual immunostaining for HP 1γ (green) and TIN2 (red) in growth-arrested 184 cells cultured as a monolayer on plastic. Arrowheads indicate overlapping (yellow) HP 1 staining and large TIN2 domains. Nuclei were counterstained with DAPI (blue). Size bars = 5 microns.

Fig. 4. Formation of large TIN2 domains is independent of telomeres and TRF proteins. (A) HMECs (strain 184) were cultured as a monolayer on plastic and growth-arrested before fixation and dual staining for TIN2 (red) and telomeres (PNA FISH; green) (upper panels), TIN2 (red) and TRF1 (green) (middle panels), and TIN2 (red) and TRF2 (green) (lower panels). (B) Higher magnification images of dual staining for TIN2 (red) and TRF2 (green) showing co-localization at small foci (yellow), indicating telomeric localization. Nuclei were counterstained with DAPI (blue). Arrowheads indicate large TIN2 domains. Size bars = 5 microns.

Fig. 5. Formation of large TIN2 domains correlates with exit from the cell cycle. (A) Percentage of S1 cells with large TIN2 domain(s) and Ki-67 staining. S1 cells were cultured in 3-D for 3 days to obtain a mixed population of cycling (Ki-67 positive; Ki-67+) and growth-arrested (Ki-67 negative, Ki-67-) cells, and then fixed and dual immunostained for TIN2 and Ki-67. Shown is the percentage of cells containing large TIN2 domains [TIN2 clusters] and Ki-67 positive (filled bars) or negative (open bars) staining. Error bars show the standard error of the means for three different experiments. *$p<0.001$. (B) Dual immunostaining for TIN2 (green) and Ki-67 (red) in

S1 cells after 3-D culture for 3 days. The different phases of the cell cycle were identified by the pattern of Ki-67 staining. The percentage of cells showing large TIN2 domains [TIN2 clusters] in each phase of the cell cycle is given below each panel, and is the average of three different experiments +/-standard error of the mean. Arrowheads indicate large TIN2 domains and dashed-lines delineate the nuclear periphery. Size bar = 2.5 microns. (C) Histogram of the percentage of synchronized HMECs (strain 184) with large TIN2 domains [TIN2 clusters] as a function of the cell cycle. Nuclei showing large TIN2 domains were counted as a percentage of total nuclei (revealed by DAPI counterstaining) during exponential (EXP), G0, S, and G2/M phases of the cell cycle. Percentages of Ki-67 positive nuclei in each phase are shown.

Fig. 6. TIN2 controls growth arrest in mammary epithelial cells. (A) Schematic of wild type TIN2 (WT TIN2), and N-terminally (TIN2-13) and C-terminally (TIN2-15) truncated forms of TIN2. (B) Expression of TIN2 and TIN2-13 in control and TIN2-13 expressing cells shown on western blot images. Lanes: cells used for infection (control), cells expressing TIN2-13 (TIN2-13), cells infected with insertless vector (control vector), cells overexpressing wild type TIN2 (TIN2), control HT1080 fibroblasts expressing exogenous TIN2 and TIN2-13 (TIN2 +TIN2-13 mixture in HT1080). Arrows indicate the location of the respective bands for TIN2 and TIN2-13. Beta-catenin is used as a loading control. (C) TIN2-15 expression in monolayer and 3-D culture shown by anti-myc immunostaining (green). Nuclei were counterstained with DAPI. (D) Vector control, TIN2-13 and TIN2-15 infected S1 cells were cultured in 3-D for 10 days. Shown are phase contrast images of acini formed by vector control S1 cells and abnormal looking colonies formed by TIN2-13 and TIN2-15 S1 cells. The arrows indicate enlarged and/or irregular multicellular structures. (E) Non-infected S1 cells [control] and vector control, TIN2-13, or TIN2-15 infected S1 cells were cultured in 3-D for 10 days. Acini were classified according to

six diameter ranges (6-15 μm, 16-25 μm, 26-35 μm, 36-45 μm, 46-55 μm, 56-65 μm). Shown is the percentage of acini in each diameter range out of a total of 400 acini observed in each independent experiment. Three experiments were performed. (F) Immunostaining for the endogenous BM component collagen IV (red) and Ki-67 (green) in vector control or TIN2-15 S1 cells cultured in 3-D for 10 days. When proper morphogenesis occurs, acini are surrounded by a continuous BM and > 90% of the cells arrest proliferation. One nucleus positive for Ki-67 is seen out of 10 nuclei in vector control; 5 nuclei positive for Ki-67 are seen out of 14 nuclei in TIN2-15. Arrows indicate the absence of collagen IV around part of the TIN2-15 colony. (G) GFP-S1 cells organized in an acinus [left panel]. Immunostaining for the endogenous BM component collagen IV (red) [central panel] and α6-integrin (green) and beta-catenin (red) [right panel] in hTERT-expressing S1 cells cultured in 3-D for 10 days. When proper morphogenesis occurs, in addition to the continuous BM, acini display the localization of α6-integrin at the basal cell membrane (against the BM) and beta-catenin at cell-cell junctions. (H) Immunostaining for TIN2 (red) in control or TIN2-15 S1 cells. In the control acinus, 8 of 9 nuclei, identified by DAPI staining, have a large TIN2 domain (arrowheads). In the acinar structure formed by TIN2-15-expressing cells, 4 of 13 nuclei show one or two large TIN2 domains (arrowheads) and one nucleus shows completely fragmented TIN2 domains (arrow). Size bars = 25 microns.

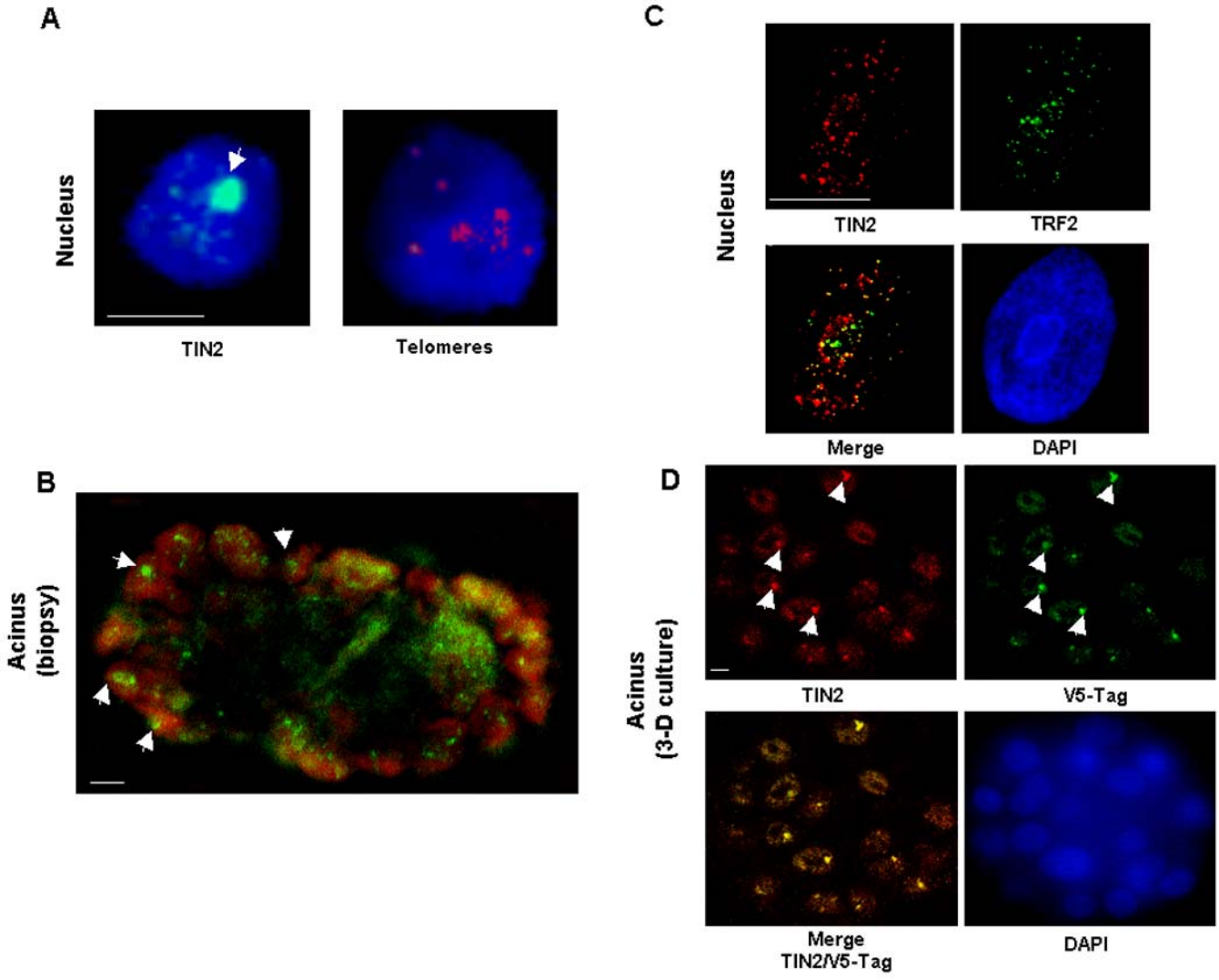
A
Nucleus
TIN2
Telomeres
B
Acinus
(biopsy)
C
Nucleus
TIN2
TRF2
Merge
DAPI
D
Acinus
(3-D culture)
TIN2
V5-Tag
Merge
TIN2/V5-Tag
DAPI

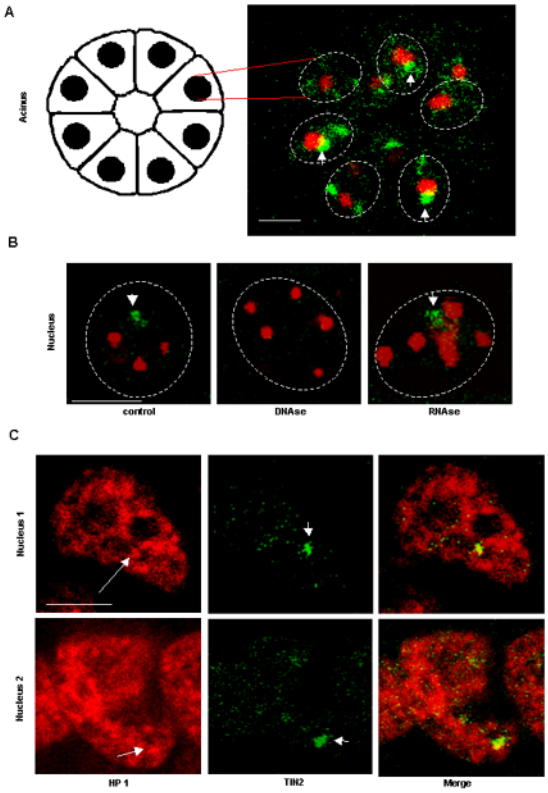
A
Acinus
B
Nucleus
control
DNAse
RNAse
C
Nucleus 1
Nucleus 2
HP 1
TIN2
Merge

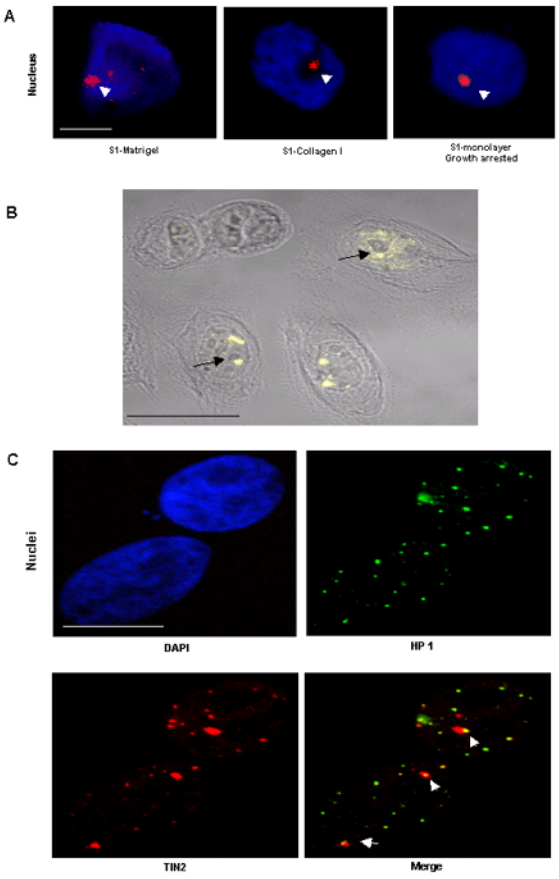
A
Nucleus
S1-Matrigel
S1-Collagen I
S1-monolayer
Growth arrested
B
C
Nuclei
DAPI
HP 1
TIN2
Merge

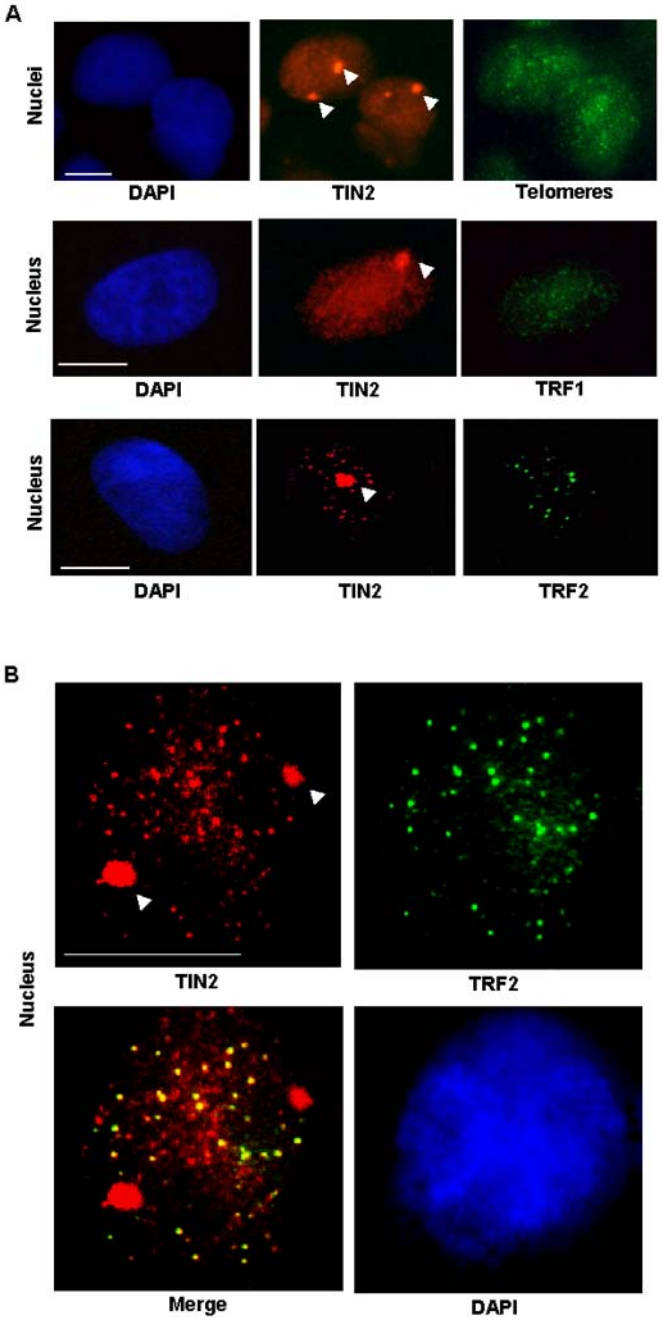
A
Nuclei
DAPI
TIN2
Telomeres
Nucleus
DAPI
TIN2
TRF1
Nucleus
DAPI
TIN2
TRF2
B
Nucleus
TIN2
TRF2
Merge
DAPI

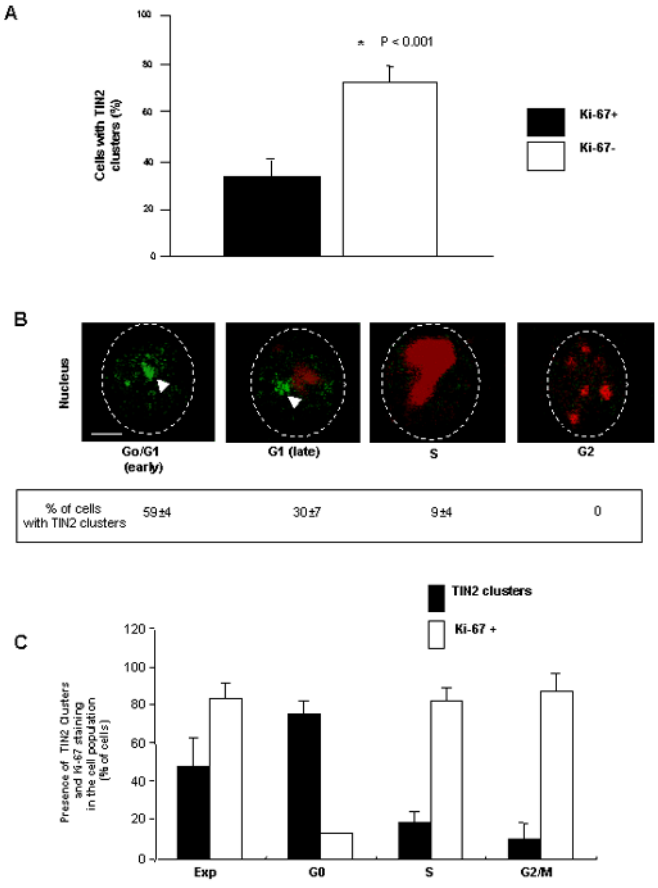
A
Cells with TIN2 clusters (%)
100
80
60
40
20
0
* P < 0.001
Ki-67+
Ki-67-
B
Nucleus
Go/G1 (early)
G1 (late)
S
G2
% of cells with TIN2 clusters
59±4
30±7
9±4
0
C
TIN2 clusters
Ki-67 +
Presence of TIN2 Clusters and Ki-67 staining in the cell population (% of cells)
120
100
80
60
40
20
0
Exp
G0
S
G2/M

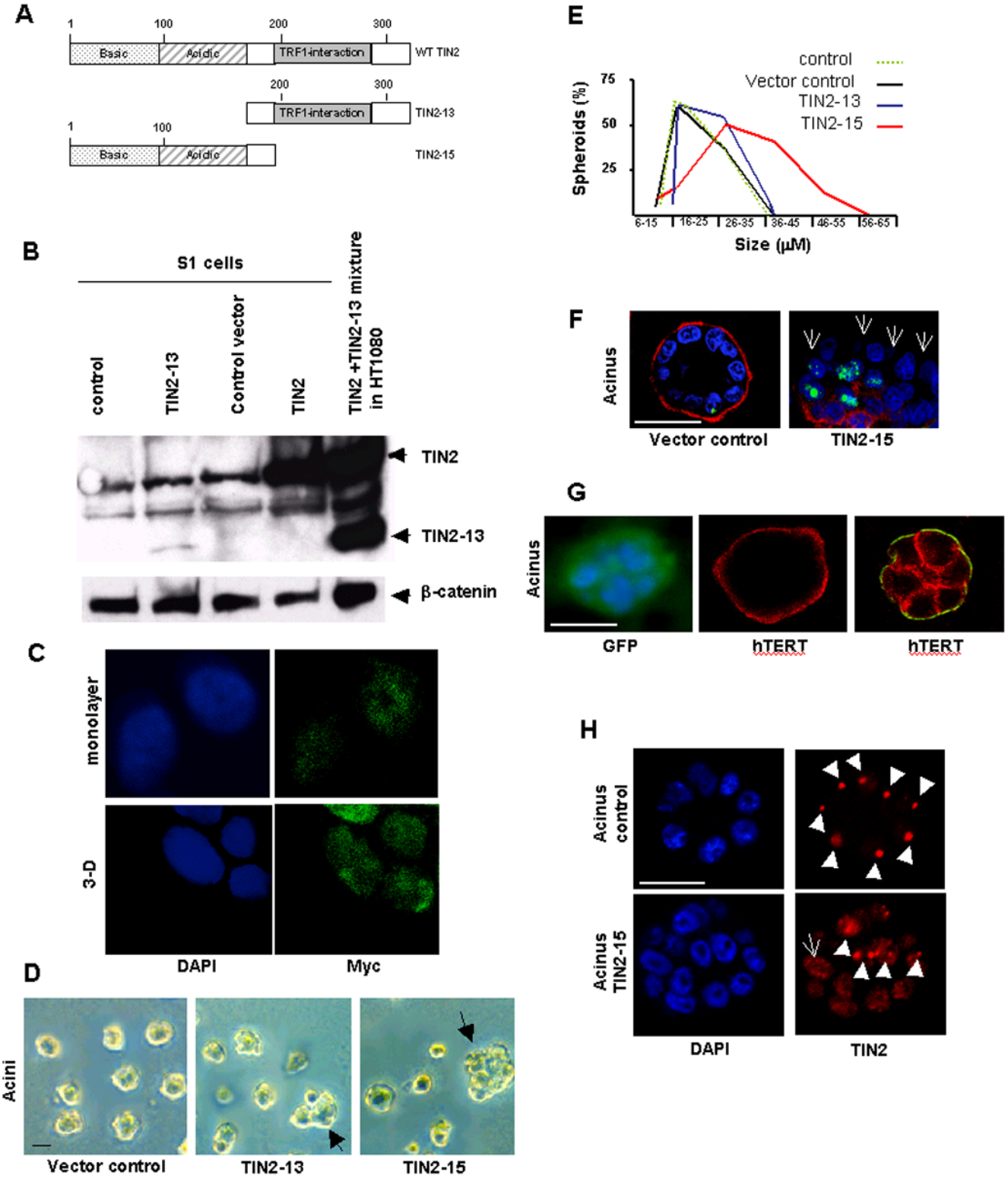
A
1
100
200
300
Basic
Acidic
TRF1-interaction
WT TIN2
TIN2-13
TIN2-15
B
S1 cells
control
TIN2-13
Control vector
TIN2
TIN2 +TIN2-13 mixture in HT1080
TIN2
TIN2-13
β-catenin
C
monolayer
3-D
DAPI
Myc
D
Acini
Vector control
TIN2-13
TIN2-15
E
control
Vector control
TIN2-13
TIN2-15
Spheroids (%)
75
50
25
6-15
16-25
26-35
36-45
46-55
56-65
Size (μM)
F
Acinus
Vector control
TIN2-15
G
Acinus
GFP
hTERT
hTERT
H
Acinus control
Acinus TIN2-15
DAPI
TIN2